SIMS proceedings paper

SURFACE and INTERFACE ANALYSIS

Received: 6 October 2011 Revised: 19 January 2012 Accepted: 25 May 2012 Published online in Wiley Online Library: 9 July 2012

(wileyonlinelibrary.com) DOI 10.1002/sia.5077

An experimental and theoretical view of energetic C_{60} cluster bombardment onto molecular solids

Daniel A. Brenes,[a] Zbigniew Postawa,[b] Andreas Wucher,[c] Paul Blenkinsopp,[d] Barbara J. Garrison[a] and Nicholas Winograd[a]*

Recent experimental measurements and calculations performed by molecular dynamics computer simulations indicate, for highly energetic C_{60} primary ions bombarding molecular solids, the emission of intact molecules is unique. An energy- and angle-resolved neutral mass spectrometer coupled with laser photoionization techniques was used to measure the polar angle distribution of neutral benzo[a]pyrene molecules desorbed by 20-keV C_{60}^+ primary ions and observed to peak at off-normal angles integrated over all possible emission energies. Similarly, computer simulations of 20-keV C_{60} projectiles bombarding a coarse-grained benzene system resulted in calculations of nearly identical polar angle distributions. Upon resolving the measured and calculated polar angle distributions, sputtered molecules with high kinetic energies are the primary contributors to the off-normal peak. Molecules with low kinetic energies were measured and calculated to desorb broadly peaked about the surface normal. The computer simulations suggest the fast deposition of energy from the C_{60} impact promotes the molecular emission by fluid-flow and effusive-type motions. The signature of off-normal emission angles is unique for molecules because fragmentation processes remove molecules that would otherwise eject near normal to the surface. Experimental measurements from a Ni {001} single crystal bombarded by 20-keV C_{60}^+ demonstrate the absence of this unique signature. Copyright © 2012 John Wiley & Sons, Ltd.

Keywords: fluid-flow desorption; effusive desorption; angular distribution; EARN; C60 sputtering; tof-snms photoionization

Introduction

Over the past few years, the employment of cluster ion beams such as SF_5, Au_3, Bi_3, and C_{60} in secondary ion mass spectrometry (SIMS) experiments has proven to be tremendously advantageous over atomic ion beams. These advantages associated with the use of cluster ion beams in SIMS experiments are known to stem from fundamental differences in the sputtering process. Early experiments that subjected a solid surface to energetic cluster impacts indicated that a nonlinear or nonadditive enhancement of the sputtering or ejected yield occurs which is not observed with energetic atomic ion beams.[1,2] Analytical descriptions and molecular dynamics (MD) computer simulations have indicated the root cause of the nonlinear enhancement in sputtering yield is associated with the cluster impact depositing energy into a relatively confined space resulting in a region with a high density of energy.[3,4]

Very few fundamental experiments that probe the interaction of C_{60} ion beams with solid surfaces have been performed. Increased atomic and molecular sputtering yields have been demonstrated both experimentally and theoretically, but the details regarding the emission mechanism remain to be fully understood. In this paper, the mechanism of molecular emission due to energetic C_{60} cluster bombardment is determined by experimentally measuring the trajectories of energy- and angle-resolved neutral (EARN) molecules desorbed from a molecular solid by 20-keV C_{60} bombardment and then compared to trajectories calculated on a closely related system by MD computer simulations. The comparison reveals that molecular desorption occurs by two distinct mechanisms which are manifested as anisotropic polar angle distributions. These mechanisms include a fluid-flow process at higher kinetic energies,[5,6] and an effusive-type desorption at lower kinetic energies.[7] Even though different molecules are used in comparing experiment and theory, previous simulations have shown that the sputtering dynamics of various molecules is similar under C_{60} bombardment.[6,8–11] Unlike C_{60} sputtered atoms from metals, fragmentation processes of molecules minimize the ejection of molecules about the surface normal. The findings presented are important for providing a fundamental understanding of the C_{60} cluster/molecular solid interaction.

Experimental and computational methods

Experimental

Benzo[a]pyrene (b[a]p, $C_{20}H_{12}$, Sigma-Aldrich Chemical Co.) was physically vapor deposited onto a substrate, while the thickness

* *Correspondence to: Nicholas Winograd, The Pennsylvania State University, Department of Chemistry, University Park, PA 16802, USA. E-mail: nxw@psu.edu*

a *The Pennsylvania State University, Department of Chemistry, University Park, PA, 16802, USA*

b *Smoluchowski Institute of Physics, Jagiellonian Univeristy, ul. Reymonta 4, 30-059 Krakow, Poland*

c *Faculty of Physics, University of Duisburg-Essen, 47048 Duisburg, Germany*

d *Ionoptika Ltd., Epsilon House Chilworth Science Park, Southampton SO53 4NF, U.K.*

was monitored using a quartz crystal microbalance (TM-400, Maxtek, Inc.). Verification with an atomic force microscope (Nanopics 2100, TLA Tencor Inc.) confirmed a 400-nm thickness with an RMS surface roughness of 2 nm. There are a few reasons why b[a]p was experimentally investigated. One, molecular films are readily prepared by physical vapor deposition,[12] resulting in a amorphous structure with a uniform thickness large enough to avoid substrate effects.[13] Two, the photoionization cross section is large enough to achieve the necessary sensitivity, and the rigidity of the molecule lessens the probability of photodissociation.[13–16] Three, the size of the molecule is the largest to be investigated experimentally concerning the mechanism of molecular emission.

For comparison to an atomic system, a Ni {001} single crystal was chosen and analyzed in similar experimental conditions. The Ni single crystal was optically polished and oriented to within $\pm 0.5^\circ$ of the {001} surface plane. For this comparison, the surface of the crystal was extensively cleaned by a series of cycles that involved sputter cleaning with an 8-keV Ar^+ ion source delivering 15 μA for 30 min and followed by annealing at 920 K for 30 min. Flashing the crystal to 1100 K resulted in a bright and sharp (1×1) LEED pattern.[17]

The experiments were carried out in a time-of-flight mass spectrometer which uses a position sensitive detector to collect EARN distributions of sputtered material from solid surfaces subjected to energetic ion beams. A full description of the EARN mass spectrometer can be found elsewhere,[18] but the instrumental updates are discussed for this experiment. The EARN is equipped with a fullerene ion source (Ionoptika, Ltd.) capable of delivering 25 nA of C_{60}^+ ions accelerated to 20 keV. A 200-ns pulse of C_{60}^+ ions was used to bombard at normal incidence the b[a]p film. A Nd:YAG-pumped dye laser (Lambda-Physik ScanMate Pro) producing 280 nm[14] of light with 6-ns pulses and focused into a ribbon was used to photoionize the sputtered neutral species. An EARN distribution is measured by recording the mass-selected signal amplitude for b[a]p as a function of position on the detector and time delay between the firing of the C_{60} ion source and the laser pulse. The b[a]p film was cooled to 85 K with liquid nitrogen cooled nitrogen gas, to reduce the contribution of gas phase molecules and previously observed thermal effects in molecular sputtering.[19,20] All gas phase background signals were subtracted from each EARN distribution. In a similar fashion, the EARN distributions for sputtered Ni atoms were collected by implementing a multi-photon resonant ionization scheme to detect Ni atoms in the excited state.[21] A more thorough analysis detailing the emission process for C_{60} sputtered Ni atoms from a single crystal is in preparation.

Computational details

Buckminster fullerene bombardment onto a benzene crystal was simulated by MD to calculate kinetic energy, polar angle distributions (not shown), and cross-sectional views of sputtered and relocated material. The impact energy for C_{60} was set to 20 keV along with an impact angle of 0°. The benzene crystal was arranged as follows: (i) a hemispherical radius of 25.7 nm, (ii) maintained at a temperature of 0 K via a heat bath composed of rigid and stochastic molecules. There are three main factors that limited the simulated system to be benzene. First, the benzene crystal is designed to speed up the computational time by means of coarse-graining approximations (CGA). In CGA, hydrogen atoms are combined with their nearest-bonded carbon atom into a bead identified as CH.[22] Within the scope of this investigation, benzene will be referred to as coarse-grained (cg-) benzene. Second, being that benzene is a smaller molecule, a higher intact molecular yield is obtained that ensures statistically significant energy, and angular distributions are calculated. Third, benzene is the fundamental building block for b[a]p. Although there are differences in the overall structure of both systems, the comparison to one another is justified as discussed below.

Results and discussion

The experimental and calculated kinetic energy distributions are shown in Fig. 1a. What is significant from this energy distribution is that the peak position is a reflection of the system's cohesive energy. In this particular investigation, b[a]p cohesive energy is approximately 2.5 times larger than molecular benzene,[23] and so the maxima for Fig. 1a are reasonable. However, as shown in Fig. 1b, the energy distributions are corrected for the cohesive energy of the system by plotting the normalized signal intensities

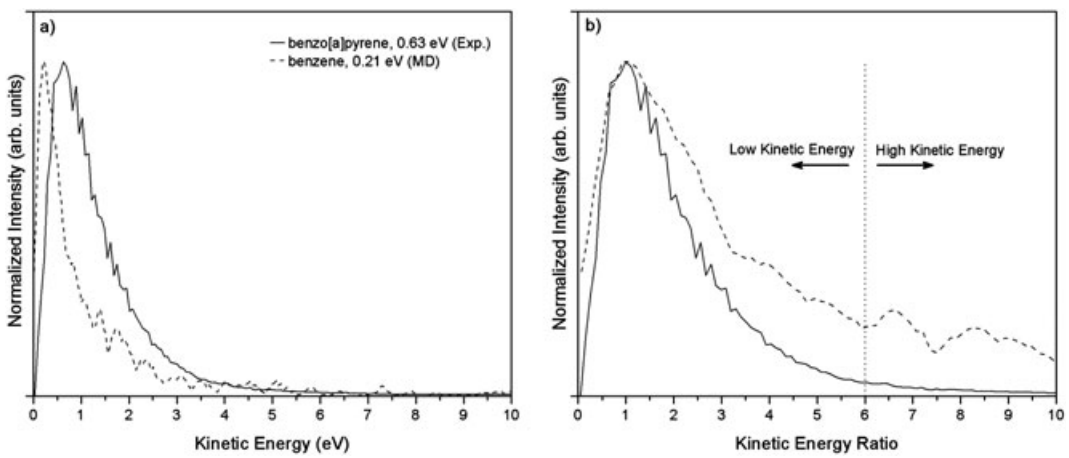

Figure 1. a) The kinetic energy distribution for neutral intact benzo[a]pyrene molecules (solid line, experiment) and coarse-grained benzene molecules (dash line, calculated) desorbed by 20-keV C_{60} projectiles with an impact angle of 0° to the surface normal. b) The kinetic energy distribution corrected for the cohesive energy by defining the abscissa as a ratio of the molecule's kinetic energy to the peak position, 0.63 eV for benzo[a]pyrene and 0.21 eV for coarse-grained benzene.

as a function of the ratio between the kinetic energy of the sputtered molecule to the respective peak position. The main purpose for the correction is to define a dividing energy, as indicated by the dotted vertical line in Fig. 1b, to distinguish sputtered molecules with low kinetic energies from those with high kinetic energies when plotting the polar angle distribution. In turn, with the appropriate position, this allows the optimization of the anisotropy in the polar angle distributions as discussed below.

The experimental polar angle distribution for ejected neutral b[a]p molecules is shown in Fig. 2. In addition, the integrated kinetic energy polar angle distribution is energy-resolved into two distributions representing b[a]p molecules desorbed with low and high kinetic energy. The limit used to split the integrated polar angle distribution was determined by the position of the vertical line in Fig. 1b, the dividing energy. It should be noted, the position of the vertical line is a ratio; however, it translates into an optimal dividing energy for b[a]p molecules at 3.8 eV. Discussed below are the mechanisms for molecular emission that give rise to the features in Fig. 2.

The b[a]p energy integrated polar angle distribution shown in Fig. 2 highlights a peak positioned at an emission angle of approximately 30° and overlaid onto a near over-cosine background. The energy-resolved polar angle distribution would suggest that: one, there is a significant contribution from off-normal emission that consists mainly of high energy b[a]p molecules; and two, the near over-cosine background is comprised of b[a]p molecules with low emission energies. In addition, the polar angle distribution for C_{60} sputtered Ni atoms from a Ni {001} single crystal indicate atoms primarily emit about the surface normal as shown in Fig. 2. Although not shown, the Ni atom energy-resolved angular distribution does not reveal any signs of off-normal emission. As previously mentioned, details of the sputtering process for Ni atoms from a single crystal is in preparation. Nevertheless, differences in the polar angle distributions between molecules and atoms suggest the emission process for molecules is not the same.

Calculations performed on the cg-benzene system can provide insights into the emission mechanism that governs the off-normal emission of neutral b[a]p molecules in Fig. 2. To begin, a side view of all sputtered, relocated cg-benzene molecules and fragments from their original position within the target are shown in Fig. 3a. It is clear the C_{60} impact induced the formation of four distinct zones. These zones are comprised of sputtered molecules and fragments, as well as relocated and unperturbed molecules. Nearest the point of impact is the fragmentation core (red zone), in which complete molecular fragmentation occurs, thus ejecting only fragments primarily about the surface normal (red arrow). However, directly beneath the point of impact, some molecules are sputtered but the majority of molecules are ejected with off-normal angles (green arrow) from a region (green zone) that surrounds the fragmentation core.

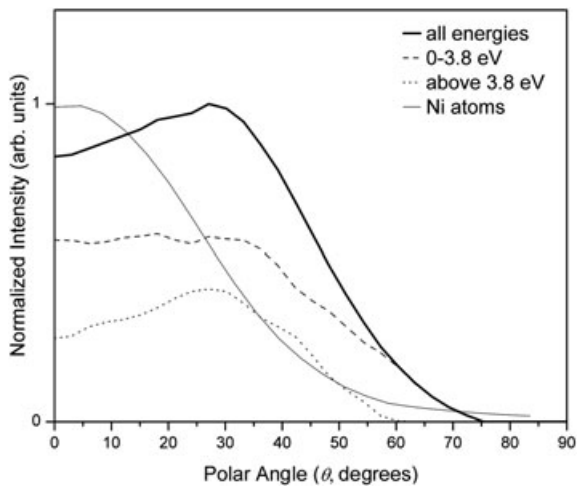

Figure 2. The experimental polar angle distribution of benzo[a]pyrene molecules and Ni atoms desorbed by 20-keV C_{60} primary ions. The normalized signal intensity is plotted *versus* the emission angle and as a function of emission energy; benzo[a]pyrene molecules with all energies (solid), 0–3.8 eV (dash), above 3.8 eV (dot) and Ni atoms with all emission energies (solid, thin line).

Resolving the side view into top views as a function of ejected cg-benzene kinetic energy provides further insights into the mechanism responsible for molecular emission. Top views of sputtered cg-benzene molecules, with either less than or above 1.26 eV of kinetic energy (determined via vertical line in Fig. 1b), are shown in Figs. 3b, 3c. Molecules that are ejected with kinetic energies above 1.26 eV are sputtered from a ring-like zone and originated from the first four layers (1–2 nm) as the crater develops. The ring-like zone indicates the absence of molecules ejected about the surface normal, thus giving rise to the anisotropic polar angle distribution. Upon the swift C_{60} penetration and disintegration into carbon atoms, the fragmentation core is created which resides centrally within the ring-like zone. An outward and lateral expansion of the core causes an upward sweeping motion of intact molecules with off-normal angles from the surface. This molecular motion matches those from previous simulations,[5,6,10,11] and therefore can be characterized as molecular emission by fluid flow. As the core expands, collisions between the carbon atoms and fragments lead to the emission of fragments along the surface normal, with few sputtered molecules. For atomic solids, these energetic particles emitted in a normal direction would be the same as those emitted off-normal, and the angular distribution would appear as over-cosine (Fig. 2a, Ni atoms). Therefore, the presence of the off-normal peak in the polar angle distribution is also a reflection of molecular fragmentation.

On the other hand, the top view of cg-benzene molecules ejected with kinetic energies less than 1.26 eV indicates they are removed from top and deep layers ($>$ 5 nm) from the crater. It should be emphasized the expansion of the fragmentation core is complete, the crater is fully developed, and the fluid-flow ceases to continue. However, the emission of intact molecules and fragments continue due to effusive-type motions.[7] Only interactions between weakly bound fragments and intact molecules along the walls of the fully developed crater cause an effusive-type desorption of weakly bound intact molecules with very low kinetic energies and emission angles that are over-cosine.

Conclusions

In summary, from the experimental measurements and the theoretical predictions presented, it is highly suggested the sputtering processes involved in the ejection of intact molecules by energetic C_{60} cluster bombardment are not the same when compared to the bombardment of a metallic surface. In the case of an organic surface, the process involves a swift C_{60} impact at the surface leaving an energized region primarily composed of molecular fragments. Expansion of this region stimulates molecular desorption at off-normal angles and high kinetic energy by

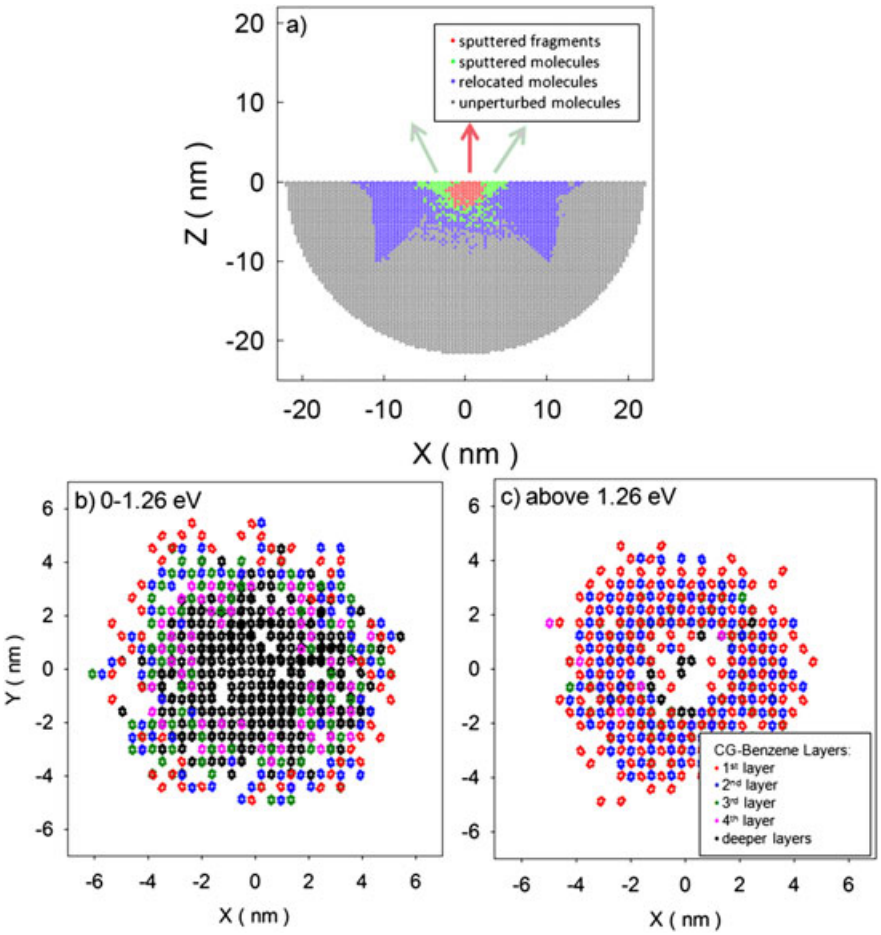

Figure 3. Top and cross-sectional views of the cg-benzene system upon 20-keV C_{60} bombardment. a) Cross-sectional view of all sputtered, relocated molecules and fragments. Top views of b) molecules sputtered with kinetic energies of 0–1.26 eV and c) molecules sputtered with kinetic energies above 1.26 eV. Note in the cross-sectional view Y = 0 nm and in the top view Z = 0 nm.

means of fluid flow. Upon expansion of the region, molecules with low kinetic energy begin to desorb over all angles due to effusive-type motions. In the case of a clean metallic surface, fragmentation does not occur, and so atoms predominantly eject in the near-normal direction.

Acknowledgements

The authors gratefully acknowledge financial support from the National Institute of Health Grant No. 2R01 EB002016-18, the National Science Foundation Grant Nos. CHE-0908226 and CHE-0910564, the Department of Energy Grant No. DE-FG02-06ER15803, and the Polish Ministry of Science and Higher Education Program No. N N204 183940.

References

[1] D. A. Thompson, S. S. Johar, *Appl. Phys. Lett.* **1979**, *34*, 342–345.
[2] D. A. Thompson, S. S. Johar, *Radiat Eff. Defects Solids* **1981**, *55*, 91–98.
[3] H. M. Urbassek, *Top Appl Phys* **2007**, *110*, 189–230.
[4] B. J. Garrison, Z. Postawa, *Mass Spectrom. Rev.* **2008**, *27*, 289–315.
[5] M. F. Russo, B. J. Garrison, *Anal. Chem.* **2006**, *78*, 7206–7210.
[6] B. J. Garrison, Z. Postawa, K. E. Ryan, J. C. Vickerman, R. P. Webb, N. Winograd, *Anal. Chem.* **2009**, *81*, 2260–2267.
[7] T. J. Colla, R. Aderjan, R. Kissel, H. M. Urbassek, *Phys. Rev. B.* **2000**, *62*, 8487–8493.
[8] A. Delcorte, B. J. J. Garrison, *Phys. Chem. C.* **2007**, *111*, 15312–15324.
[9] R. Paruch, L. Rzeznik, B. Czerwinski, B. J. Garrison, N. Winograd, Z. Postawa, *J. Phys. Chem. C* **2009**, *113*, 5641–5648.
[10] M. F. Russo, C. Szakal, J. Kozole, N. Winograd, B. J. Garrison, *Anal. Chem.* **2007**, *79*, 4493–4498.
[11] K. E. Ryan, B. J. Garrison, *Anal. Chem.* **2008**, *80*, 6666–6670.
[12] D. Willingham, A. Kucher, N. Winograd, *Appl. Surf. Sci.* **2008**, *255*, 831–833.
[13] R. Chatterjee, D. E. Riederer, Z. Postawa, N. J. Winograd, *Phys. Chem. B* **1998**, *102*, 4176–4182.
[14] D. M. Hrubowchak, M. H. Ervin, N. Winograd, *Anal. Chem.* **1991**, *63*, 225–232.
[15] C. A. Meserole, E. Vandeweert, Z. Postawa, N. Winograd, *J. Phys. Chem. B* **2004**, *108*, 15686–15693.
[16] C. L. Brummel, K. F. Willey, J. C. Vickerman, N. Winograd, *Int. J. Mass Spectrom. Ion Processes* **1995**, *143*, 257–270.
[17] C. Xu, J. S. Burnham, S. H. Goss, K. Caffey, N. Winograd, *Phys. Rev. B.* **1994**, *49*, 4842–4849.
[18] P. H. Kobrin, G. A. Schick, J. P. Baxter, N. Winograd, *Rev. Sci. Instrum.* **1986**, *57*, 1354–1362.
[19] C. Lu, A. Wucher, N. Winograd, *Anal. Chem.* **2011**, *83*, 351–8.
[20] L. L. Zheng, A. Wucher, N. Winograd, *Anal. Chem.* **2008**, *80*, 7363–7371.
[21] C. He, Z. Postawa, S. Rosencrance, R. Chatterjee, B. J. Garrison, N. Winograd, *Phys. Rev. Lett.* **1995**, *75*, 3950–3953.
[22] E. J. Smiley, Z. Postawa, I. A. Wojciechowski, N. Winograd, B. J. Garrison, *Appl. Surf. Sci.* **2006**, *252*, 6436–6439.
[23] M. V. Roux, M. Temprado, J. S. Chickos, Y. Nagano, *J. Phys. Chem. Ref. Data* **2008**, *37*, 1855–1996.

